AFRL-RX-WP-TR-2012-0310

WATER-SOLUBLE NANODIAMOND (POSTPRINT)

John Jones
Thermal Sciences & Materials Branch

Oleksandr Kuznetsov, Yanqiu Sun, Ryan Thaner, Ariana Bratt, Varun Shenoy, Michael S. Wong, and W.E. Billups
Rice University

MARCH 2012
Interim

AIR FORCE RESEARCH LABORATORY
MATERIALS AND MANUFACTURING DIRECTORATE
WRIGHT-PATTERSON AIR FORCE BASE, OH 45433-7750
AIR FORCE MATERIEL COMMAND
UNITED STATES AIR FORCE

NOTICE AND SIGNATURE PAGE

Using Government drawings, specifications, or other data included in this document for any purpose other than Government procurement does not in any way obligate the U.S. Government. The fact that the Government formulated or supplied the drawings, specifications, or other data does not license the holder or any other person or corporation; or convey any rights or permission to manufacture, use, or sell any patented invention that may relate to them.

Qualified requestors may obtain copies of this report from the Defense Technical Information Center (DTIC) (http://www.dtic.mil).

AFRL-RX-WP-TP-2012-0310 HAS BEEN REVIEWED AND IS APPROVED FOR PUBLICATION IN ACCORDANCE WITH ASSIGNED DISTRIBUTION STATEMENT.

//SIGNED//
JOHN JONES, Program Manager
Thermal Sciences and Materials Branch
Materials and Manufacturing Directorate

//SIGNED//
NADER HENDIZADEH, Branch Chief
Thermal Sciences and Materials Branch
Materials and Manufacturing Directorate

//SIGNED//
SHASHI K. SHARMA, Deputy Chief
Nonmetallic Materials Division
Materials and Manufacturing Directorate

This report is published in the interest of scientific and technical information exchange, and its publication does not constitute the Government's approval or disapproval of its ideas or findings.

REPORT DOCUMENTATION PAGE

Form Approved
OMB No. 0704-0188

1. REPORT DATE *(DD-MM-YY)*	2. REPORT TYPE	3. DATES COVERED *(From - To)*
March 2012	Technical Paper	1 October 2008 – 1 March 2012

4. TITLE AND SUBTITLE
WATER-SOLUBLE NANODIAMOND (POSTPRINT)

5a. CONTRACT NUMBER
In-house

5b. GRANT NUMBER

5c. PROGRAM ELEMENT NUMBER
62102F

6. AUTHOR(S)
John Jones (AFRL/RXBT)
Oleksandr Kuznetsov, Yanqiu Sun, Ryan Thaner, Ariana Bratt, Varun Shenoy, Michael S. Wong, and W.E. Billups (Rice University)

5d. PROJECT NUMBER
4347

5e. TASK NUMBER

5f. WORK UNIT NUMBER
BT109202

7. PERFORMING ORGANIZATION NAME(S) AND ADDRESS(ES)
Thermal Sciences and Materials Branch
Nonmetallic Materials Division
Air Force Research Laboratory, Materials and Manufacturing Directorate
Wright-Patterson Air Force Base, OH 45433-7750
Air Force Materiel Command, United States Air Force

Rice University

8. PERFORMING ORGANIZATION REPORT NUMBER
AFRL-RX-WP-TR-2012-0310

9. SPONSORING/MONITORING AGENCY NAME(S) AND ADDRESS(ES)
Air Force Research Laboratory
Materials and Manufacturing Directorate
Wright-Patterson Air Force Base, OH 45433-7750
Air Force Materiel Command
United States Air Force

10. SPONSORING/MONITORING AGENCY ACRONYM(S)
AFRL/RXBT

11. SPONSORING/MONITORING AGENCY REPORT NUMBER(S)
AFRL-RX-WP-TR-2012-0310

12. DISTRIBUTION/AVAILABILITY STATEMENT
Approved for public release; distribution unlimited.

13. SUPPLEMENTARY NOTES
The U.S. Government is joint author of this work and has the right to use, modify, reproduce, release, perform, display, or disclose the work. PA Case Number and clearance date: 88ABW-2012-1190, 6 March 2012. This document contains color.

14. ABSTRACT
Nanodiamond particles possess extraordinary mechanical, electronic, thermal, and tribological properties and exhibit significant potential as components of novel multifunctional materials. However, processing of diamond nanoparticles for many applications is hampered by agglomeration and inhomogeneous dispersions in organic or aqueous solvents that are often used for these applications. The search for novel methods to process nanodiamonds is thus an important goal in materials science. In this study, we report a versatile, scalable synthesis of water-soluble nanodiamonds using a route similar to that demonstrated earlier for carbon nanotubes and graphene.

15. SUBJECT TERMS
water soluble, nanodiamond, chemical processing

16. SECURITY CLASSIFICATION OF:			17. LIMITATION OF ABSTRACT:	NUMBER OF PAGES	19a. NAME OF RESPONSIBLE PERSON (Monitor)
a. REPORT	b. ABSTRACT	c. THIS PAGE			John Jones
Unclassified	Unclassified	Unclassified	SAR	10	19b. TELEPHONE NUMBER *(Include Area Code)* N/A

Langmuir

Article

pubs.acs.org/Langmuir

Water-Soluble Nanodiamond

Oleksandr Kuznetsov,[†] Yanqiu Sun,[‡] Ryan Thaner,[‡] Ariana Bratt,[‡] Varun Shenoy,[§] Michael S. Wong,[§] John Jones,[∥] and W. E. Billups*[,‡]

[†]Department of Physics, Rice University, 6100 Main Street, Houston, Texas 77005, United States

[‡]Department of Chemistry and The Richard E. Smalley Institute for Nanoscale Science and Technology, Rice University, 6100 Main Street, Houston, Texas 77005, United States

[§]Department of Chemical and Biomolecular Engineering, Rice University, 6100 Main Street, Houston, Texas 77005, United States

[∥]Air Force Research Laboratory, Materials and Manufacturing Directorate, Thermal Sciences and Materials Branch, 2941 Hobson Way, Wright-Patterson AFB, Ohio 45433, United States

Supporting Information

ABSTRACT: Reduction of the graphenic edges of annealed nanodiamond by sodium in liquid ammonia leads to a nanodiamond salt that reacts with either alkyl or aryl halides by electron transfer to yield radical anions that dissociate spontaneously into free radicals and halide. The free radicals were observed to add readily to the aromatic rings of the annealed nanodiamond. Nanodiamonds functionalized by phenyl radicals were sulfonated in oleum, and the resulting sulfonic acid was converted to the sodium salt by treatment with sodium hydroxide. The solubility of the salt in water was determined to be 248 mg/L. Nanodiamond functionalized by carboxylic acid groups could be prepared by reacting 5-bromovaleric acid with the annealed nanodiamond salt. The solubility of the sodium carboxylate in water was found to be 160 mg/L.

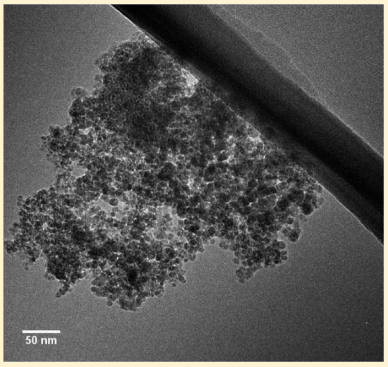

1. INTRODUCTION

Nanodiamond particles possess extraordinary mechanical, electronic, thermal, and tribological properties and exhibit significant potential as components of novel multifunctional materials.[1−9] However, processing of diamond nanoparticles for many applications is hampered by agglomeration and inhomogeneous dispersions in organic or aqueous solvents that are often used for these applications. The search for novel methods to process nanodiamonds is thus an important goal in materials science.[10−18] In this study, we report a versatile, scalable synthesis of water-soluble nanodiamonds using a route similar to that demonstrated earlier for carbon nanotubes[19] and graphene.[20]

2. EXPERIMENTAL SECTION

2.1. Materials. Nanodiamond powder (98% purity, particle size 3−5 nm) prepared by detonation was received from NanoAmor Inc. (Houston, Texas). The nanodiamond was annealed by heating under argon in a quartz tube furnace at 1100 °C for 3 h. The annealing step also eliminates, in part, material that forms on the surface of the nanodiamond during production and processing.[21−26]

2.2. General Procedures for the Functionalization Reactions. *Synthesis of Carboxylated Nanodiamond* ***2***. Annealed nanodiamond **1** (100 mg) was added under argon to a flame-dried 100 mL three-neck round-bottomed flask equipped with a stir bar and fitted with a condenser. The flask was placed in a cooling bath, and ammonia (60 mL) was then condensed into the flask. Sodium (1.9 g, 10 equiv) was then added. After 30 min, 5-bromovaleric acid (6 g, 4 equiv) was added to the flask, and the cooling bath was removed. Dry ice was added to the condenser for 4 h, and the ammonia was allowed to evaporate overnight. The reaction mixture was quenched with ethanol and filtered through a 0.2 μm PTFE membrane. Finally, the material was washed several times with water and ethanol. The functionalized nanodiamond was then dried overnight at 80 °C.

Synthesis of Carboxylated Nanodiamond Salt ***3***. The sodium salt was prepared by treating the functionalized nanodiamond **2** with 1 M NaOH (60 mL) at 80 °C for 24 h. The resulting salt was filtered through a PTFE membrane, washed with water, and dried overnight at 80 °C.

Synthesis of Phenylated Nanodiamond ***4***. Phenylation experiments were performed by adding the graphitized nanodiamond **1** (100 mg) to a dry 100 mL, three-neck, round-bottomed flask equipped with a stirring bar and fitted with a dry ice condenser. All reactions were carried out under an atmosphere of argon. A cooling bath was used to condense ammonia (60 mL) into the flask. Sodium (1.9 g, 10 equiv) was then added, and after 30 min iodobenzene (3.7 mL, 4 equiv) was added and the cooling bath was removed. The mixture was then stirred for 4 h. The ammonia was allowed to evaporate overnight. The reaction mixture was quenched with ethanol and filtered through a 0.2 μm PTFE membrane. Finally, the material was washed several times with ethanol and once with chloroform. The phenylated nanodiamond was dried overnight.

Synthesis of Sulfonated Nanodiamond ***5***. Sulfonation was carried out under argon by dispersing the phenylated nanodiamond **4** (60 mg) in oleum (60 mL) in a dry 100 mL three-neck round-bottomed flask with a reflux condenser. The mixture was heated at 80 °C for 4 h. The suspension was then added to 300 mL of ice water, filtered through a 0.2 μm PTFE membrane, and washed with water.

Received: November 25, 2011
Revised: February 22, 2012
Published: February 23, 2012

   dx.doi.org/10.1021/la204660h | *Langmuir* 2012, 28, 5243−5248

Synthesis of Sulfonated Nanodiamond Salt **6**. The phenyl sulfonated nanodiamond **5** was treated with 1 M NaOH solution (60 mL) overnight at 80 °C. The resulting mixture was separated on a centrifuge.

2.3. Solubility Measurements in Water. Solubility measurements of the functionalized nanodiamond samples were performed as follows: 100 mg of the functionalized material was dispersed in 100 mL of DI water and sonicated for 20 min; the dispersion was then left to settle for 1 day. The top 50 mL of solution was then decanted and filtered through the pre weighed 0.2 μm PTFE membrane, dried at 80 °C in the oven overnight. The collected sample and membrane were then weighed. The weight of the membrane was deducted to determine the weight of the sample that was dissolved.

2.4. Characterization. Starting and functionalized materials were characterized by Raman spectroscopy, Fourier transform infrared spectroscopy (FTIR), thermogravimetric analysis (TGA), X-ray photoelectron spectroscopy (XPS), high-resolution transmission electron microscopy (HRTEM), and high-contrast transmission electron microscopy (HC-TEM). Raman spectra were collected using a Renishaw 1000 micro-Raman system with a 514 nm laser source. FTIR spectra were obtained using a Nicolet spectrometer with the ATR accessory. TGA data were obtained using a model SDT 2960 TA Instruments in an atmosphere of argon. Samples were dried at 100 °C for 10 min and then heated at 10 °C/min to 800 °C. XPS data were obtained using a physical electronics (PHI QUANTERA) XPS/ESCA system. The base pressure was at 5×10^{-9} Torr. A monochromatic Al X-ray source at 100 W was used with pass energy of 26 eV and with a 45° takeoff angle. The beam diameter was 100.0 μm. Powder X-ray diffraction (XRD) spectra were collected using a Rigaku D/max Ultima II Powder Diffractometer. Three separate locations were analyzed for each sample. HRTEM images were recorded using a high-resolution transmission electron microscope (HRTEM, JEM-2010F) operated at an accelerating voltage of 200 kV. HC-TEM images were taken using high contrast transmission electron microscope (JEOL 1230 HC-TEM) operated at 100 kV.

The size of the nanodiamond clusters stabilized in DI water, reported as hydrodynamic diameter D_h, was measured using a Brookhaven ZetaPALS DLS instrument equipped with a He−Ne laser (λ = 656 nm) and a BI-9000AT digital autocorrelator. All measurements were conducted at room temperature using standard 4 mL polystyrene cuvettes at a fixed scattering angle of 90°. The measurements were conducted multiple times for each sample to ensure reliability of data. The diameters reported are number-weighted which were obtained using the CONTIN fitting algorithm. Volume-weighted hydrodynamic diameter ($D_{h,v}$) values were determined and compared to the number-weighted D_h values. Since number-weighted diameters vary as D_h and volume-weighted diameters vary as D_h^3, the case of $D_{h,v} \approx D_h$ indicates a narrow size distribution and the case of $D_{h,v} > D_h$ indicates the additional presence of larger-diameter particles. For all three nanodiamond samples in which particle size analysis was performed by DLS, $D_{h,v}$ was found to be larger than D_h (vide infra): $d_{h,v}$ = 283 ± 15, 703 ± 50, and 553 ± 45 nm for sample **3**, sample **6** at pH 7, and sample **6** at pH 14, respectively. Excluding the largest particles (<5% of the total population), the remaining cluster population in each sample had $d_{h,v}$ values of 189 ± 12, 443 ± 42, and 170 ± 21 nm, respectively. These values are similar to the D_h values (vide infra), and thus D_h can be taken to represent the average diameter of >95% of the cluster population for a given nanodiamond suspension.

3. RESULTS AND DISCUSSION

Commercially available detonation nanodiamond obtained as a dark gray hydrophobic powder was used for this study. A preliminary study of the nanodiamond was carried out by recording the high-resolution transmission electron microscopy image shown in Figure 1. The image was recorded by dropping a suspension of the nanodiamond from chloroform onto a lacey carbon grid. The lattice structure of the nanodiamond can be observed clearly in the TEM image. Since the nanodiamond was prepared by detonation synthesis[25,26] the image also shows

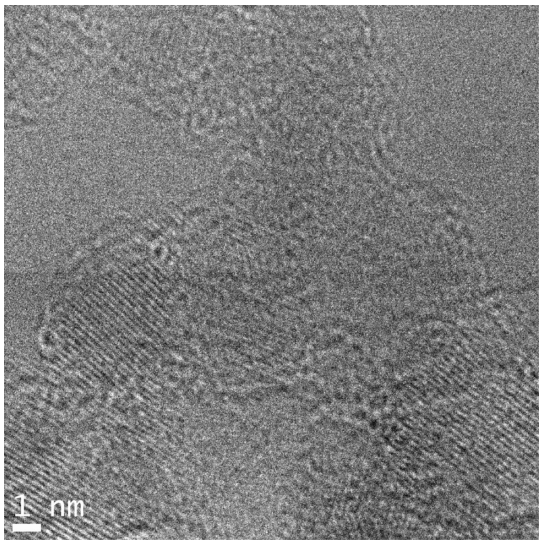

Figure 1. High-resolution transmission electron microscopy (HRTEM) image of detonation nanodiamond showing fringes. The image was recorded by dropping a suspension of the nanodiamond in chloroform onto a lacey carbon grid.

a large amount of material bound to the edges of the agglomerated nanodiamond. These groups are thought to be composed primarily of oxygen containing groups that are introduced by acid treatment during the purification process. The agglomerization results from attachment of the nanodiamond particles through chemical bonds that result from intermolecular reactions of the edge groups.[10]

The functionalization schemes that we have used to affect solubility have their genesis in our earlier work on the functionalization of carbon nanotubes[19] and graphene.[20] The salient feature of this work involves electron transfer from an alkali metal to the aromatic rings of the nanocarbon. Since nanodiamonds are void of aromatic rings, it was necessary to carry out an annealing step that adds a few layers of graphene to the edges of the nanodiamond. Nanodiamond graphitization is a well studied process.[21−24] In our hands, heating the nanodiamond to 1100 °C for 3 h proved to be sufficient to add the required layers of graphenic material (Chart 1). The graphene can be seen clearly in the HRTEM image shown in Figure 2. An XPS survey analysis of the annealed nanodiamond **1** gave the carbon content as 98.8% and the oxygen content as 1.2%.

Chart 1. Surface Graphitization of Detonation Nanodiamond

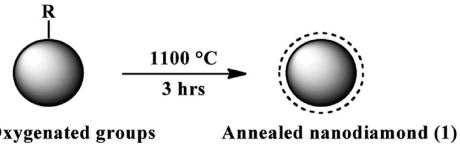

The survey and high resolution images are shown in the Supporting Information as SI-1a and SI-2a.

Graphitization was also demonstrated by XRD. The XRD spectra of samples annealed at 700, 900, and 1100 °C are presented in Figure 3b−d, respectively. The intensity of the diamond peaks decreases concomitantly as a broad diffraction peak at 2θ = 23° corresponding to graphitic carbon appears. Samples graphitized at 1100 °C were used for these studies.

dx.doi.org/10.1021/la204660h | *Langmuir* 2012, 28, 5243−5248

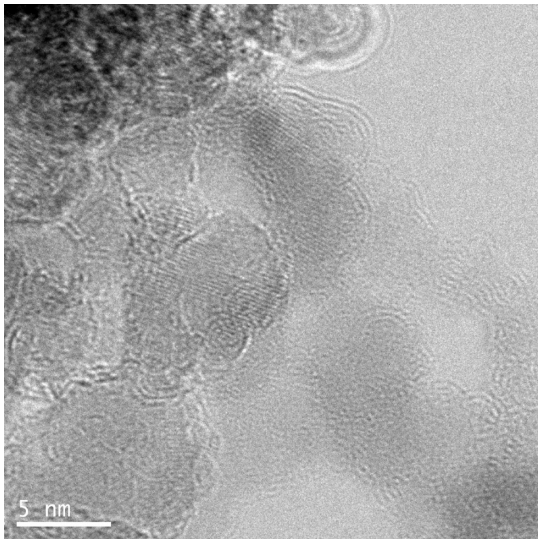

Figure 2. High resolution transmission electron microscopy (HRTEM) image of detonation nanodiamond showing layers of graphene.

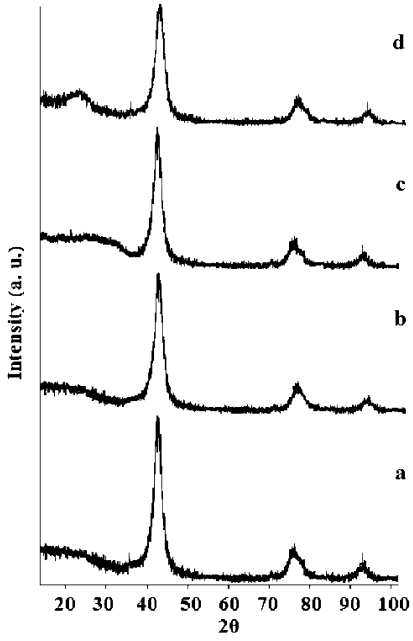

Figure 3. XRD spectra of the pristine nanodiamond (a) and nanodiamond annealed at 700 (b), 900 (c), 1100 °C (d). Peaks at 2θ = 43°, 75°, and 91° correspond to (111), (220), and (311) diamond planes, respectively. The broad peak at 2θ = 25° is (002) graphite plane.

Raman spectra of the raw pristine detonation nanodiamond and the nanodiamond annealed at 1100 °C are presented in Figure 4, panels a and b, respectively. The annealed nanodiamond exhibits prominent peaks corresponding to the disorder D band at 1330 cm^{-1} and the G band at 1570 cm^{-1}. The appearance of these bands demonstrates the formation of a graphitic structure.

An FTIR spectrum of the pristine nanodiamond shows the presence of hydroxyl groups (broad peak around 3400 cm^{-1}) and a cluster of carbonyl peaks at 1600 cm^{-1} (Figure 5a). The annealed nanodiamond does not exhibit these absorptions (Figure 5b).

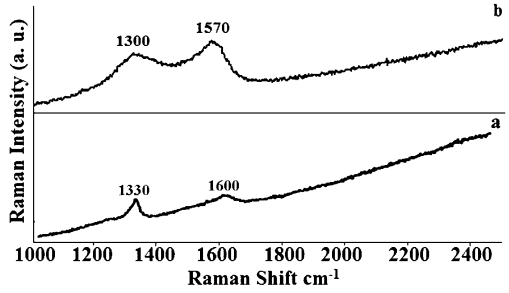

Figure 4. Raman spectra of (a) pristine nanodiamond, (b) nanodiamond annealed at 1100 °C for 3 h.

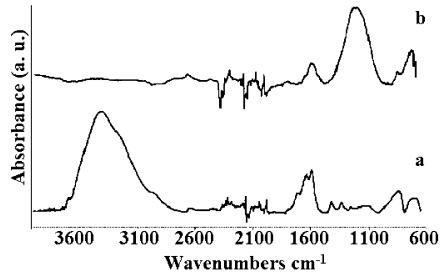

Figure 5. FTIR spectra of (a) pristine nanodiamond and (b) annealed nanodiamond.

The reactions that have been used to functionalize the annealed nanodiamond are illustrated in Scheme 1. Thus reduction of the graphenic edges of the annealed nanodiamond by sodium in liquid ammonia leads to the nanodiamond salt **1.** This material can be reacted with either alkyl or aryl halides to yield a radical anion that dissociates spontaneously into a radical and halide. The free radicals add readily to the aromatic rings of the annealed nanodiamond.

When 5-bromovaleric acid was added to a suspension of **1** in liquid ammonia, **2** was obtained as a moderately water-soluble material. Further treatment of **2** with NaOH yields the sodium salt **3**. These reactions are outlined in Scheme 2. Solubility of the salt **3** in water was determined to be 160 mg/L. A suspension of **3** in water is stable for several months. The annealed nanodiamond exhibits no solubility in water.

The sample **3** was found to have a hydrodynamic diameter D_h of 182 ± 9 nm. A high contrast TEM image of the functionalized nanodiamond cluster is shown in Figure 6. The size of a typical cluster, as shown in the image, is approximately 200 nm, in good agreement with the hydrodynamic diameter measured by DLS.

TGA data are presented in Figure 7 showing almost no weight loss for the starting annealed nanodiamond upon heating to 800 °C under argon (curve 1). Curves 2 and 3 represent functionalized samples **2** and **3** (scheme 1) and show weight losses of 30% and 32%, respectively.

XPS analysis serves to corroborate the composition of **2** and **3.** These survey analyses are shown in the Supporting Information as SI-1b and SI-1c. The high resolution scan for **3** is shown in the Supporting Information as SI-2b. The FTIR spectrum of **2** exhibits a broad O−H peak centered at 3400 cm^{-1} and C−H stretching peaks at 2850 and 2930 cm^{-1}.

A more soluble product could be obtained when the annealed nanodiamond was functionalized by phenyl sulfonate groups (as the sodium salt), a protocol that has been used

dx.doi.org/10.1021/la204660h | *Langmuir* 2012, 28, 5243−5248

Scheme 1. Functionalization Reactions of Annealed Nanodiamond

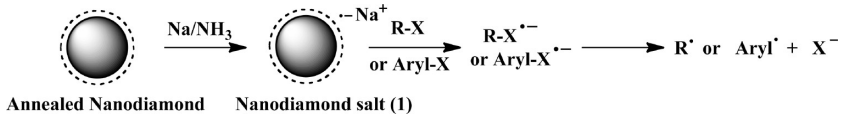

Scheme 2. Synthesis of Water-Soluble Nanodiamonds 2 and 3

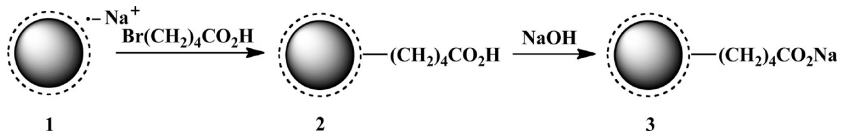

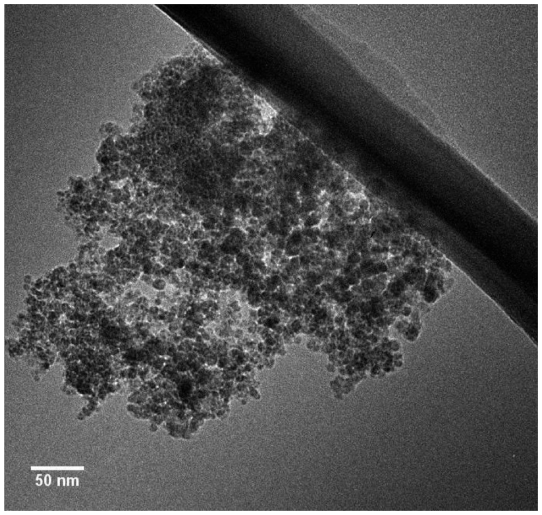

Figure 6. High contrast transmission electron microscopy image of the sodium salt **3**. The scale bar is set to 50 nm.

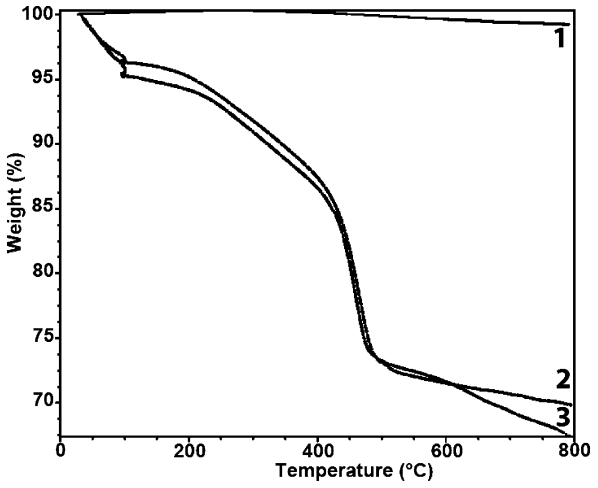

Figure 7. Thermal gravimetric analyses: annealed nanodiamond (curve 1), carboxylated nanodiamond **2** (curve 2), and sodium salt **3** of carboxylated nanodiamond **2** (curve 3).

previously to prepare soluble carbon nanotubes and graphene. The syntheses are illustrated in Scheme 3. The phenyl radicals that form from the iodobenzene radical anion (Scheme 1) add readily to the annealed nanodiamond to give **4**. Sulfonation of **4** by oleum and conversion to the sodium salt **6** proved to be uneventful. High resolution TEM image of the sulfonated nanodiamond **5** indicates no structural changes and demonstrates that fringes are present in the diamond region (SI-3).

The solubility of **6** in water was determined to be 248 mg/L. Solubilities found for water-soluble nanodiamond samples are lower than some values reported elsewhere.[27] In our opinion, the more conservative approach to solubility measurements used in this work accounts for this result.

The XPS survey and high resolution spectra are presented in the Supporting Information as SI-1d and SI-2c. Elemental analysis shows presence of carbon, oxygen (13.3%), sulfur (1.1%), and sodium (3.2%). At high pH a stable suspension is obtained. This protocol has been used previously to prepare water-soluble solutions of carbon nanotubes[19] and graphene[20] that can be kept for several years without any appreciable precipitation.

Thermal gravimetric analyses of nanodiamond samples **4** and **5** are shown in Figure 8. Curve 1 demonstrates the negligible weight loss of the starting material in comparison with curve 2 that shows a 24% weight loss for phenylated nanodiamond **4**. Curve 3 shows thermal degradation of the sulfonated product **5** (Scheme 3) where the weight loss was determined to be 33%. Due to the hydrophilic nature of the functionalized material, the initial weight loss (up to 100 °C) may be related to desorption of water from the surface of nanoparticles.

DLS measurements in water at pH 7 and 14 indicated the hydrodynamic diameter D_h of functionalized nanodiamond **6** to be 420 ± 30 nm and 164 ± 7 nm, respectively. These values are consistent with high-contrast TEM analysis. The TEM image revealed cluster sizes in the same range for **6** deposited from aqueous solutions of pH 7 and 14 (Figure 9, panels a and b).

Infrared spectra of **4**–**6** are presented in Figure 10. Sulfonic acid groups (Figure 10b) show a broad absorption at ~1200 cm^{-1}, confirming the presence of the sulfonic acid (ν_{S-O} and $\nu_{S\text{-phenyl}}$).[20]

Future studies will include an evaluation of the thermal properties of these materials.

Scheme 3. Synthesis of Water-Soluble Nanodiamonds 5 and 6

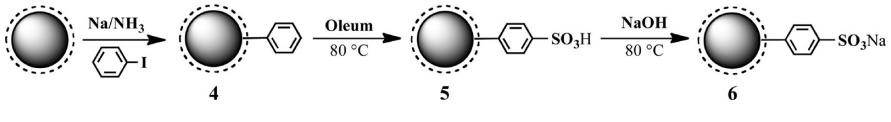

dx.doi.org/10.1021/la204660h | Langmuir 2012, 28, 5243–5248

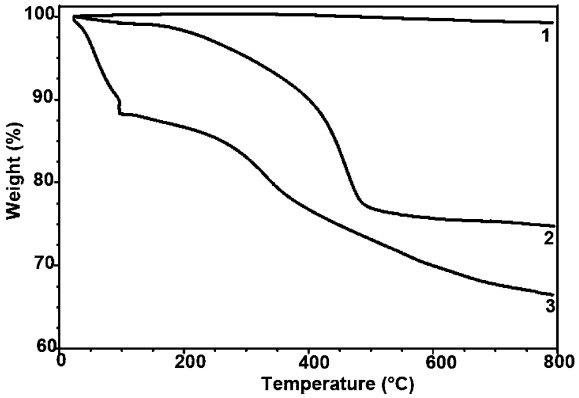

Figure 8. Thermal gravimetric analyses: annealed nanodiamond (curve 1), phenylated nanodiamond **4** (curve 2), and sulfonated nanodiamond **5** (curve 3).

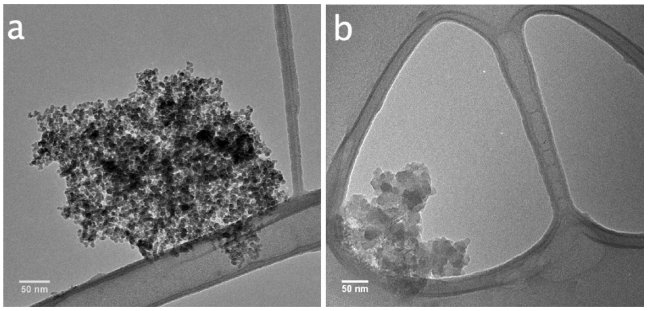

Figure 9. High contrast-transmission electron microscopy image of the sodium salt **6** deposited from (a) a neutral aqueous solution and (b) a highly alkaline solution.

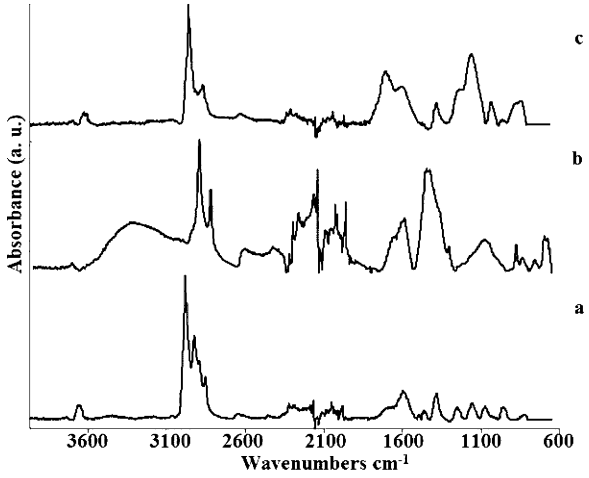

Figure 10. FTIR spectra of (a) phenylated nanodiamond (product **4**), (b) sulfonated phenyl nanodiamond (product **5**), and (c) sodium salt of the sulfonated phenyl nanodiamond (product **6**).

■ ASSOCIATED CONTENT

Supporting Information

Detailed descriptions of the XPS and the high resolution TEM image of water-soluble nanodiamond **5**. This material is available free of charge via the Internet at http://pubs.acs.org.

■ AUTHOR INFORMATION

Corresponding Author

*E-mail: billups@rice.edu. Tel.: 713-348-5694.

Notes

The authors declare no competing financial interest.

■ ACKNOWLEDGMENTS

We gratefully acknowledge the Robert A. Welch Foundation (C-0490) for support of this work. We thank Dr. G. C. Kini for fruitful discussions.

■ REFERENCES

(1) Khabashesku, V. N.; Margrave, J. L.; Barrera, E. V. Functionalized carbon nanotubes and nanodiamonds for engineering and biomedical applications. *Diamond Relat. Mater.* **2005**, *14*, 859−866.

(2) Kurmashev, V. I.; Timoshkov, Y. V.; Orehovskaja, T. I.; Timoshkov, V. Y. Nanodiamonds in magnetic recording system technologies. *Phys. Solid State* **2004**, *46*, 696−702.

(3) Yu, Y.-C.; Huang, J.-H.; Lin, I.-N. Electron field emission properties of nanodiamonds synthesized by the chemical vapor deposition process. *J. Vac. Sci. Technol. B* **2001**, *19*, 975−980.

(4) Bondar, V. S.; Pozdnyakova, I. O.; Puzyr, A. P. Applications of nanodiamonds for separation and purification of proteins. *Phys. Solid State* **2004**, *46*, 758−760.

(5) Vaijayanthimala, V.; Chang, H.-C. Functionalized fluorescent nanodiamonds for biomedical applications. *Nanomedicine* **2009**, *4*, 47−55.

(6) Mochalin, V. N.; Gogotsi, Y. Wet chemistry route to hydrophobic blue fluorescent nanodiamond. *J. Am. Chem. Soc.* **2009**, *131*, 4594−4595.

(7) Wu, Y. Y.; Tsui, W. C.; Liu, T. C. Experimental analysis of tribological properties of lubricating oils with nanoparticle additives. *Wear* **2007**, *262*, 819−825.

(8) Lee, J.-Y.; Lim, D.-S. Tribological behavior of PTFE film with nanodiamond. *Surf. Coat. Technol.* **2004**, *188−189*, 534−538.

(9) Williams, O. A.; Nesladek, M.; Daenen, M.; Michaelson, S.; Hoffman, A.; Osawa, E.; Haenen, K.; Jackman, R. B. Growth, electronic properties and applications of nanodiamond. *Diamond Relat. Mater.* **2008**, *17*, 1080−1088.

(10) Krueger, A. The structure and reactivity of nanoscale diamond. *J. Mater. Chem.* **2008**, *18*, 1485−1492.

(11) Liu, Y.; Gu, Z.; Margrave, J. L.; Khabashesku., V. N. Functionalization of Nan scale Diamond Powder: Fluoro-, Alkyl-, Amino and Aminoacid-Nanodiamond Derivatives. *Chem. Mater.* **2004**, *16*, 3924−3930.

(12) Chang, I. N.; Hwang, K. C.; Ho, J. A.; Lin, C.-C.; Reuben, J.-R.; Horng, H. J.-A. Facile Surface Functionalization of Nanodiamonds. *Langmuir* **2010**, *26*, 3685−3689.

(13) Li, L.; Davidson, J. L.; Lukehart, C. M. Surface functionalization of nanodiamond particles via atom transfer radical polymerization. *Carbon* **2006**, *44*, 2308−2315.

(14) Lora Huang, L.-C.; Chang, H.-C. Adsorption and Immobilization of Cytochrome *c* on Nanodiamonds. *Langmuir* **2004**, *20*, 5879−5884.

(15) Chao, J.-I.; Perevedentseva, E.; Chung, P.-H.; Liu, K.-K.; Cheng, C.-Y.; Chang, C.-C.; Cheng, C.-L. Nanometer-Sized Diamond Particle as a Probe for Biolabeling. *Biophys. J.* **2007**, *93*, 2199−2208.

(16) Krueger, A.; Stegk, J.; Liang, Y.; Lu, L.; Jarre, G. Biotinylated Nanodiamond: simple and efficient functionalization of detonation diamond. *Langmuir* **2008**, *15*, 4200−4204.

(17) Liang, Y.; Ozawa, M.; Krueger, A. A general procedure to functionalize agglomerating nanoparticles demonstrated on nanodiamond. *ACS Nano* **2009**, *3*, 2288−2296.

(18) Jarre, G.; Liang, Y.; Betz, P.; Liang, D.; Krueger, A. Playing the surface game − Diels-Alder reactions on diamond nanoparticles. *Chem. Commun.* **2010**, *47*, 544−546.

(19) Liang, F.; Beach, J. M.; Rai, P. K; Guo, W.; Hauge, R. H.; Pasquali, M.; Smalley, R. E.; Billups, W. E. Highly Exfoliated Water-Soluble Single-Walled Carbon Nanotubes. *Chem. Mater.* **2006**, *18*, 1520−1524.

(20) Mukherjee, A.; Kang, J. H.; Kuznetsov, O.; Sun, Y.; Thaner, R.; Bratt, A. S.; Lomeda, J. R.; Kelly, K. F.; Billups, W. E. Water-soluble

graphite nanoplatelets formed by oleum exfoliation of graphite. *Chem. Mater.* **2011**, *23*, 9−13.
(21) Butenko, Yu. V.; Kuznetsov, V. L.; Paukshtis, E. A.; Stadnichenko, A. I.; Mazov, I. N.; Moseenkov, S. I.; Boronin, A. I.; Kosheev, S. V. The thermal stability of nanodiamond surface groups and onset of nanodiamond graphitization. *Fullerenes, Nanotubes, Carbon Nanostruct.* **2006**, *14*, 557−564.
(22) Qiao, Z.; Li, J.; Zhao, N.; Shi, C.; Nash, P. Graphitization and microstructure of nanodiamond to onion-like carbon. *Scr. Mater.* **2006**, *54*, 225−229.
(23) Chen, J.; Deng, S. Z.; Chen, J.; Yu, Z. X.; Xu, N. S. Graphitization of nanodiamond powder annealed in argon ambient. *Appl. Phys. Lett.* **1999**, *74*, 3651−3653.
(24) Bogatyreva, G. P.; Voloshin, M. M.; Malogolovets, V. G.; Gvyazdovskaya, V. L.; Ilnitskaya, G. D. The effect of heat treatment on the surface condition of nanodiamond. *J. Optoelectron. Adv. Mater.* **2000**, *2*, 469−473.
(25) Daulton, T.; Eisenhour, D. D.; Bernatowicz, T. J.; Lewis, R. S.; Buseck, P. R. Genesis of presolar diamonds: comparative high-resolution transmission electron microscopy study of meteoric and terrestrial nano-diamonds. *Geochim. Cosmochim. Acta* **1996**, *60*, 4853−4872.
(26) Dolmatov, V. Detonation synthesis ultradispersed diamonds: properties and applications. *Russ. Chem. Rev.* **2001**, *70*, 607−626.
(27) Liang, Y.; Meinhardt, T.; Jarre, G.; Ozawa, M.; Vrodijak, P.; Scholl, A.; Reinhert, F.; Krueger, A. Deagglomeration and surface modification of thermally annealed nanoscale diamond. *J. Colloid Interface Sci.* **2011**, *354*, 23−30.